Partial Shading Microgeneration with Energy Storage

Leonor Mina
Instituto Superior Técnico
Universidade de Lisboa
Lisboa, Portugal
leonor.mina@tecnico.ulisboa.pt

***Abstract*—The production of electricity through distributed generation has been facing significant developments over the last years. In particular, the systems which use photovoltaic (PV) microgenerators. The main goal of this research is to design and implement a self-consumption production unit (UPAC – Unidade de Produção para Autoconsumo) able to operate under partial shading conditions (PSC). The UPAC under study operates with PV microgenerators with the integration of an energy storage system (ESS) and grid-connection. This system must supply a three-phase load located in a rural area. Therefore, it is proposed the PV structure and the design of power converters and controllers required to manage the energy involved in the system. To maximize the power extracted from the PV the backstepping algorithm is used while the three-phase inverter is controlled using sinusoidal pulse width modulation (SPWM). An ESS is developed to charge during the hours of higher solar radiation and discharge when the PV array is not able to provide the load power demand. Furthermore, a set of rules are proposed to perform the system energy management. The proposed UPAC, controllers and rules are implemented and simulated in Matlab/Simulink. Different case studies are carried out to validate the system and under PSC. Based on that, the PV power injected, load power demand, grid power and the battery state of charge are analysed.**

***Keywords* - Photovoltaic, UPAC, Energy storage, PSC, Energy management**

I. Introduction

In the last two decades, the strong worldwide development and the exponential population growth led to the increase of the demanded energy. Therefore, the concern with the search for alternatives to the use of fossil fuels has become crucial, not only because of fossil fuels scarcity, but mainly due to environmental issues [1].

Under those circumstances, the use of renewable energy sources (RES including solar, wind, hydropower, bioenergy and geothermal) in the production of energy has been a major effort for all countries. Indeed, it is estimated until 2030 that RES will represent almost 70% of the global electricity generation growth [2].

Therefore, an increasing investment has been observed in distributed generation (DG). DG consists of the production of electrical power from small energy sources up to a few tens of MW (known as microgenerators). This energy production is not originated from large power plants and its location is closer to the final consumer. DG can be grid-connected or independent of the grid [3] . A DG can include different power sources, being PV microgenerators the ones which have become the most relevant over the last years.

In Portugal, due to the high number of sunlight hours, PV technology has become a high potential field to invest. According to decree law n.º 153/2014 of October 20 an UPAC is an electricity production installation for self-consumption based on renewable or non-renewable production technologies. If the producer decides for an UPAC grid-connected, the energy not consumed can be sold to the grid at the market price. In addition, according to this decree law too, the nominal power must be equal or less than the producer/consumer (prosumer) contracted power, and the installed power equal or less than twice the nominal power [4].

Therefore, the main purpose of this work is to design and control a topology of a grid-connected UPAC (shown in Fig. 1) with the integration of an ESS and able to operate under partial shading conditions. To reach this objective the following goals were defined:

- To define a structure of PV panels connected to DC/DC converters and maximum power point tracking (MPPT) controllers to supply a three-phase load located in a rural area (see section III).
- To design decentralized controllers able to work under PSC.
- To design a storage system able to supply the load during the hours without sunlight (see section IV).
- To obtain the simulation results in different case studies. (see section V).

II. State of the Art in MPPT

The MPPT is a controller whose function is to extract the maximum power from the PV module. In order to select which algorithm to use as MPPT, Table I shows the most relevant state of the art MPPT algoritmhs.

TABLE I
MPPT Algorithms

Types of Techniques	Algorithm
Conventional	Perturb & Observe [5]
	Incremental Conductance [6]
Soft Computed	Fuzzy Logic [7]
	Artificial Neural Networks [7]
Linear	Proportional Integral Derivative [8]
Nonlinear	Backstepping

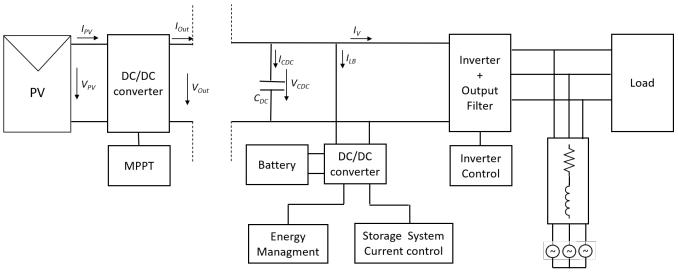

Fig. 1. Proposed topology

III. Proposed Self-Consumption Production Unit

The UPAC is designed to operate with microgenerators for self-consumption, with the integration of an ESS and grid-connection. Furthermore, considering a medium power and low voltage application, the PV array, with a peak power around 4kW, must supply a three-phase load, in Tomar.

A brief explanation of the general UPAC is made hereafter, with each block explained in more detail later:

- For the proposed approach, where partial shading conditions are considered, each PV panel is connected with its own DC/DC converter and the DC/DC output converters are series connected. Two parallel strings are used (Fig. 2 represents in detail this connection).
- Each DC/DC converter is controlled by its own MPPT. The backstepping is the algorithm selected to ensure the maximum power is extracted from the PV.
- To the DC link is also connected a battery, with its own DC/DC converter to charge/discharge.
- The battery DC/DC converter is controlled by a current control and through an energy management system (explained in detail in section IV).
- There is one DC/AC converter which allows to link an AC three-phase load and the grid. The system DC/AC converter is controlled by a voltage V_{CDC} control with internal current control.
- The grid is connected to the system through a low voltage electrical power line.

A. PV array structure

The proposed UPAC, as previously said, is designed for a PV array with peak power thereabout 4kW. Moreover, as each solar panel has 340W of rated maximum power (Table II depicts the PV data [9]) 12 PV modules are required to satisfy the load demands. In addition, considering a low voltage application 230/400V and taking into account that each panel is characterized with a maximum power point voltage of 59.7V, the PV array must be composed of two strings in parallel, each one with 6 panels connected in series (as shown Fig. 2). The total output voltage must be increased (to 700V) to limit the three-phase inverter. Since one of the objectives is to study the problem of partial shading and studying its effect on a PV system, the best approach is to consider a MPPT controller (with its DC/DC converter) for each single PV module [10]. This means that each DC/DC converter and

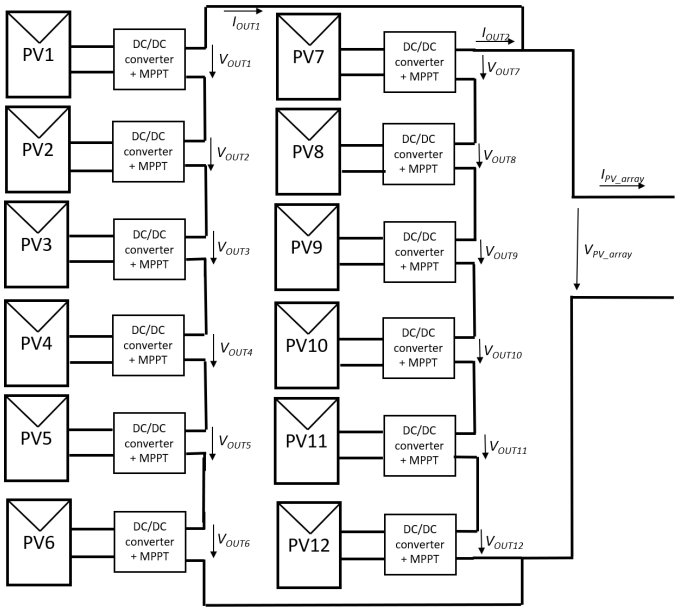

Fig. 2. PV array configuration

MPPT tracks just the maximum power point of each panel, instead of tracking a global maximum power point (GMPP) from a set of MPPs. Therefore, an algorithm to search for the GMPP is not needed. In the results it will be shown the simulation for the two structures (2 and 12 MPPTs) in order to confirm this choice.

The model used to simulate the PV module was the 1 diode 5 parameters model (1D+5P) according to [11].

TABLE II
Parameters of PV module

Parameter	Value
Rated Maximum Power (P^r_{max})	340W
Maximum Power Voltage (V^r_{mp})	59.7V
Maximum Power Current (I^r_{mp})	5.7A
Open Circuit Voltage (V^r_{oc})	71.3V
Short Circuit Current (I^r_{sc})	6.13A
Temperature Coefficient ($\mu_{V_{oc}}$)	-0.17 V/ºC
Temperature Coefficient ($\mu_{I_{sc}}$)	-3.37 mA/ºC

B. Maximum Power Point Tracking Design

In a PV system, the introduction of MPPT controllers are required since the power produced by the PV panel depends on the variation of essentially two climatic factors, such as temperature and irradiance. These two factors, which vary throughout the day, constantly change the maximum power point (MPP). Another situation, which emphasises the importance of using MPPTs, is when some of the modules are under PSC (due to trees, clouds, dirt, and other disturbances). To this end, MPPTs are introduced in order to extract the PV maximum power, under these different situations.

Therefore, the MPPT controller is connected to the DC/DC converter to adjust the switch state (ON/OFF), forcing the PV operate at MPP. First it is required to select the most suitable DC/DC converter and only after the MPPT design.

1) Buck-boost DC/DC Converter: This PV system, as stated before, is characterized to be implemented for an application of low voltage 230/400V. However, since each panel has just around 59.7V and also considering partial PV shading a DC/DC converter is required to increase the voltage. As a result, a boost converter could be used.

However, as the proposed PV structure is a PV series connection and each PV has its own MPPT converter, according to the research work in [10], the boost converter should be replaced by a buck-boost (Fig. 3). In certain periods of the day, some panels of the PV array may be under the effect of shading, thus the output voltage in those solar panels decreases. In severe shading it can happen that the output voltage of the converter decreases to very low values where the boost loses control, as its output voltage no longer higher than the input voltage, the boost converter no longer being able to set the required output voltage. Under those circumstances, the buck-boost is the most suitable converter for this proposed UPAC. Buck-boost converters have control over the output voltage, theoretically from zero to infinite, being able to deliver the MPP power regardless of the output voltage of the panel under shading conditions.

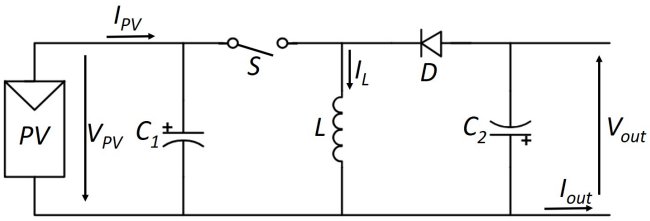

Fig. 3. Buck-boost converter

The DC/DC buck-boost converter is able of both increasing and decreasing the voltage from its input, V_{PV}, to its output, V_{out} , working as a boost and a buck, respectively. This voltage control is made controlling the duty cycle of switch *S*. The losses in capacitor C_2 are neglected, the inductor's series equivalent resistance is considered. The components C_1, L and C_2 are designed according to [12], [13] and [14], respectively.

2) Backstepping Controller Design: As a result of changing the temperature and irradiance, PV becomes a nonlinear system. To accomplish this, it is more proper to implement a nonlinear controller such as the backstepping [15]. The nonlinear backstepping controller is based on a recursive process, which depends on the appropriate choice of a Lyapunov function considering the form of control by state feedback [16], ensuring the stability and robustness of the system.

For the purpose of controlling the MPP, are considered as the controller input variables i_L, v_{PV} and i_{PV}. Accordingly, first it is calculated the reference voltage V_{PV_ref} that is the desired voltage to achieve. Afterwards, in the outer loop of the controller, the reference inductor current variable i_{L_ref} is obtained so that the voltage V_{PV} follows V_{PV_ref} (voltage control), stabilizing this subsystem [17]. In the end, the inductor current i_L is controlled (inner loop) by an hysteresis comparator, which defines the required DC/DC converter duty-cycle in order i_L to track i_{L_ref}.

First, looking in Fig. 3 the dynamic equations using the inductor volt second balance and capacitor charge balance are the following (D is the average value of the converter duty-cycle):

$$\begin{cases} \frac{dv_{pv}}{dt} = \frac{i_{pv}}{C_1} - \frac{i_L}{C_1}D \\ \frac{di_L}{dt} = \frac{v_{pv}}{L}D - \frac{v_{out}}{L}(1-D) \end{cases} \quad (1)$$

The second step is to generate the reference voltage v_{PV_ref}, of the voltage peak power, which will be then compared with the actual value v_{PV}. To do so, it is used the incremental conductance (IC) algorithm. The IC algorithm is based on analysing the slope of the PV curve. At the maximum power point $dP/dV_{PV} = 0$ which means $d(V_{PV}I_{PV})/dV_{PV} = V_{PV}(dI_{PV}/dV_{PV}) + I_{PV} = 0$. Therefore, the voltage at the maximum power point v_{PV_MPP} is:

$$v_{PV\_MPP} = -i_{PV}\frac{dv_{PV}}{di_{PV}} \quad (2)$$

The C_1 capacitor voltage v_{PV} must track a reference voltage v_{PV_ref} so that $v_{PV} = v_{PP\_ref} = v_{PV\_MPP}$. An error e_{vPV} is defined that tally to the difference between the reference value and the v_{PV_MPP} value in 2.

$$e_{vPV} = v_{PV\_ref} - v_{PV\_MPP} \quad (3)$$

To compute v_{PV_ref}, the control objective is $v_{PV\_ref} = v_{PV\_MPP}$, forcing the voltage v_{PV_ref} to track v_{PV_MPP}. This means, having zero e_{vPV}. After that, the 2nd method of Lyapunov stability is applied to ensure the stability of the equilibrium point $e_{vPV} = 0$. With this intention, it is defined a positive definite, continuously differentiable, and radially unbounded candidate Lyapunov function $V_1 = e_{vPV}^2/2$. Based on this theorem, to ensure the global asymptotic stability of the equilibrium point, the time derivative of V_1 must be definite negative $e_{vPV}de_{vPV}/dt < 0$ [18]. In order dV_1/dt to be negative,

$$\frac{de_{vPV}}{dt} = -k_{v\_MPP}e_{vPV} \quad (4)$$

where the constant k_{v_MPP} must be positive. Now, inserting 2 and 3 in 4 and bearing in mind that in the MPP the PV voltage is constant, meaning $dv_{PV\_MPP}/dt = 0$, v_{PV_ref} is given by:

$$v_{PV\_ref} = -k_{v\_MPP}\int_0^t \left(v_{PV\_ref} + i_{PV}\frac{dv_{PV}}{di_{PV}}\right)d\tau + v_{PV\_ref}(0) \quad (5)$$

From the above equation $v_{PV\_ref} + i_{PV}dv_{PV}/di_{PV} = dP_{PV}/di_{PV}$, meaning that when dP_{PV}/di_{PV} is positive, v_{PV_ref} decreases. Otherwise, when dP_{PV}/di_{PV} is negative, v_{PV_ref} increases. Hence, the v_{PV_ref} should follow v_{PV_MPP} behaviour.

The third step is to compute i_{L_ref} to control the voltage $v_{PV} = v_{PV\_ref}$. This is possible because looking for Fig. 3 $V_{C1} = V_{PV}$ and, consequently, the first equation of 1 is

$$\frac{dv_{C1}}{dt} = \frac{i_{pv}}{C_1} - \frac{i_L}{C_1} D \tag{6}$$

Defining a new error e_{vC1}:

$$e_{vC1} = v_{C1\_ref} - v_{C1} \tag{7}$$

Additionally, it is considered the integral action of the error e_{vC1} to guarantee zero steady-state error:

$$e_I = 0 \iff \int_0^t e_{vC1} d\tau = 0 \tag{8}$$

The 2nd method of Lyapunov is applied, in which the equilibrium point is $e_{vC1} = 0$. Hence, and taking account the method requirements, the candidate function is $V_2 = k_I e_I^2/2 + e_{vC1}^2/2$. To assure the global asymptotic stability:

$$\frac{dV_2}{dt} < 0 \iff k_I e_I \frac{de_I}{dt} + e_{vC1} \frac{de_{vC1}}{dt} = -k_{vC1} e_{vC1}^2 \tag{9}$$

Now, inserting equations 6, 7 and 8 in 9 the expression for the inductor reference current is received:

$$i_{L\_ref} = -\frac{C_1}{D}\left(k_{vC1} e_{vC1} + k_I \int_0^t e_{vC1} d\tau + \frac{dv_{C1\_ref}}{dt}\right) + \frac{i_{pv}}{D} \tag{10}$$

In the simulations, to compute i_{L_ref} the average duty-cycle D is defined as $D = v_{out}/(v_{PV} + v_{out})$.

The last step of the MPPT design is the current i_L control. For such, the current control uses an hysteresis comparator to define the transistor ON/OFF times (the instantaneous duty-cycle δ) to control the inductor current i_L. The output of this comparator is δ, which can take values of 0 or 1 depending if the buck-boost switch is OFF or ON, respectively. The effect of δ in controlling i_L can be explained from the second equation of 1 with $V_{C1} = V_{PV}$. Thus, the control objective is to get $i_{L\_ref} = i_L$. It is defined an error $e_{iL} = i_{L\_ref} - i_L$ which is pretended to tend to zero. It is easy to see that if $e_{iL} > 0$ then, to guarantee stability $de_{iL}/dt < 0$, implying $di_L/dt > di_{L\_ref}/dt$ and $\delta = 1$. Otherwise, if $e_{iL} < 0$ then $\delta = 0$.

To limit the switching frequency a comparator with hysteresis band between $-\Delta i_L/2 < e_{iL} < +\Delta i_L/2$ is used at variable frequency. Consequently, the switching function is:

$$\begin{cases} if \quad e_{iL} > \Delta \frac{i_L}{2} \Rightarrow \delta = 1 \\ if \quad e_{iL} < -\Delta \frac{i_L}{2} \Rightarrow \delta = 0 \end{cases} \tag{11}$$

The gains k_{v_MPP}, k_I and k_{vC1} were optimized through simulations.

C. DC/AC converter

In addition, as the PV model should supply an AC load, a DC/AC converter (inverter) is required. The inverter is a component able to convert the DC voltage to AC.

The proposed UPAC is designed for an application of medium power where the PV array peak power is around 4kW. The PV array supplies a three-phase load and is grid-tied. As a result, it must be used a three-phase inverter to inject the required AC voltage.

Fig. 4 displays the inverter topology with three legs, that match to each of the phases (k=A, B, C). In those legs are two switches that must have opposite switch positions in order to prevent short-circuit in the DC side. The inverter input filter (capacitor C_{DC}), whose function is to re-establish the voltage source characteristic at the inverter input, can be calculated in steady-state based on [12] .

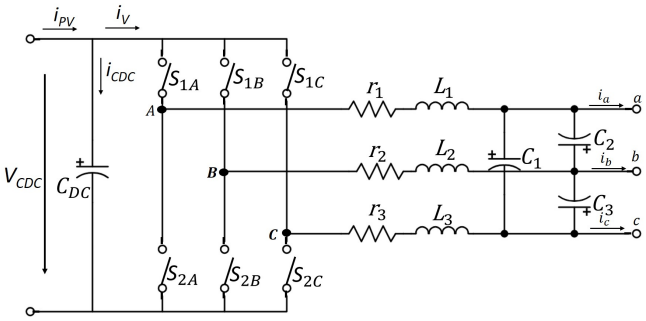

Fig. 4. Three-phase inverter

To reduce the output current total harmonic distortion (THD) an output filter is added to reduce high frequency harmonics. Thus, the inductor and capacitor (in delta connection) values are related to the ones obtained for a single-phase inverter with 3 level modulation and voltage step $V_{CDC}/3$ [19]. As the capacitors are delta connected, the value must be divided by three.

The control of the ON/OFF switches state is made resorting to a linear control, based on [20]. The control objective is to keep the input voltage V_{CDC} constant, with internal control of the inverter output currents (as shown in Fig. 5).

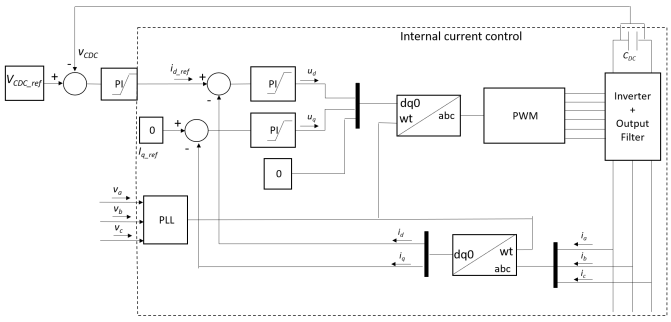

Fig. 5. Three-phase inverter system control

IV. Energy Management

This section presents all the energy management involved in the proposed UPAC. Looking for Fig. 1, the battery block with its DC/DC converter, storage system current control and energy management are responsible for this management.

When the PV array does not have enough power to supply the load, the available energy in the storage system is used. However, the UPAC is also able to answer to situations where

neither the PV nor storage system have enough power to supply the load. Thus, the connection to the grid is made in order to supply the lacking power. Moreover, the injection of energy into the grid is also considered, in cases of an excess of the power.

The ESS consists of a battery connected to a DC/DC reversible up/down converter, which controls the battery charging/discharging periods (shown in Fig. 6). Batteries take hours to recharge/discharge. However, it is not possible to simulate the whole proposed UPAC working during hours, using Simulink in a desktop/portable computer. Thus, instead of using the Simulink battery model a simple equivalent capacitor is used with a scaled capacitance to be able to observe the charge and discharged in some seconds.

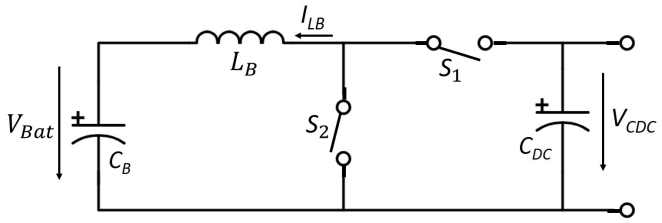

Fig. 6. Battery and DC/DC reversible buck-boost converter

The capacitor C_{DC} is the inverter input capacitor, previously explained. The component L_B can be calculated as the same way as the inductor output filter of a buck (down) converter [12]. The equivalent capacitor C_B, which is used to simulate the battery, can be roughly estimated supposing the linear part of the battery voltage ΔV when discharged at constant current I:

$$C_B = I\frac{\Delta T}{\Delta V} \tag{12}$$

To estimate I and $I\Delta T$, the total energy stored in the capacitor must be approximated as: $E = P * \Delta T$, where P will be equal to the PV array peak power and ΔT the time of charging/discharging.

The battery control is made through controlling the ON/OFF state of the switches S_1 and S_2. This control consists of two conditions, depending on whether the battery is needed or not. The energy management block (further explained) in Fig. 1 outputs a signal. This signal just takes the values 1 or 0, meaning whether the battery should supply/receive or not, respectively. In the case this signal is zero, S_1 and S_2 will be in the OFF state. When the signal is one, the battery is used (supply/receive) and controlled by a current control loop implemented to generate the signal δ_B. Thus, one of the switches is ON and the other one is OFF.

The battery current control, as depicted in Fig. 7, is implemented using a hysteresis comparator to control i_{LB}. It will make the actual battery current i_{LB} follows the reference one. When the difference between P_{PV} and P_{Load} is positive, the PV array can totally supply the load and still charge the battery. Otherwise if negative, the battery is discharging and both PV array and battery are injecting power on the load.

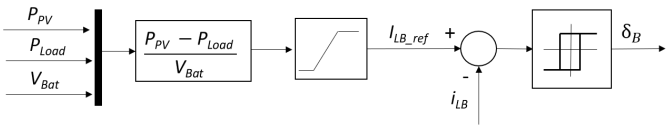

Fig. 7. Battery current control

A. Energy Management Rules

The proposed UPAC follows a set of rules maximizing the possibility to supply the load in different situations. These rules are based on the following variables:

- The PV array power injected P_{PV}.
- The demanded power by the load P_{Load}.
- The battery state of charge (SOC) in $\%\ SOC$.
- Electricity tariffs - peak, shoulder and off-peak.
- Grid codes – whether can be injected power on the grid or not.

The SOC is a relative quantity that measures the amount of energy available on a battery. Thereby, it is given by the ratio between the remaining capacity and the rated capacity [21].

Electricity tariffs define the cost an electricity consumer is charged usually per kWh (or MWh). Given the load profiles of electrical networks, tariffs usually depend on the hour of the day, on the day of the week and on the season (summer/winter). In this research work is considered a three-time-of-use, which consists of three different tariffs [22]:

- Off-peak hours: hours when the electricity consumption is cheapest.
- Shoulder hours: hours when the electricity is charged with a tariff between the one charged in off-peak and peak.
- Peak hours: hours when electricity consumption is more expensive.

The grid codes are related to whether energy can be injected into the grid or not. This means that the grid at some periods of the day may have excess energy and, hence the voltage increases. Therefore, in these situations, energy cannot be injected on the grid (grid codes are set to 0 in the rules table).

Based on this, the Table III describes the rules used to make all the system energy management. The symbol ϕ means any of the options of the respective factor. In the Simulink, this table is applied through a Matlab function block, whose input variables are P_{PV}, P_{Load}, SOC, electricity tariffs and grid-codes. The output is a signal which decides if the battery is used or not (previously explained).

Note that, rule 6th proposes to remove the PV from the MPP decreasing P_{PV}. This is required when the power injected by the PV array is higher than the power consumed by the load, the battery has $SOC = 100\%$ and the excess energy cannot be injected in the grid. Therefore, the PV operation point should be changed for a value where the PV just injects the load power demand. Removing the PV from MPP is explained in [23] - [24].

TABLE III
ENERGY MANAGEMENT RULES

	P_{PV} **relatively to** P_{Load}	**SOC %**	**Consumption Time**	**Grid Permission**	**System Response**
1	$P_{PV} > P_{P_{Load}}$	80 <SOC <100	Peak/Soulder	1	PV supplies power to the load and injects the remaining on the grid.
2				0	PV supplies power to the load. However, as the grid does not allow, the battery is charged until be totally full (100%).
3			Off-peak	ϕ	PV supplies power to the load and injects the remaining to charge the battery until to be full. Grid is not used.
4		0 <SOC <80	ϕ	ϕ	PV supplies power to the load and injects the remaining to charge the battery. Grid is not used.
5		SOC = 100	ϕ	1	PV supplies power to the load and injects the remaining on the grid (it is sold energy). Battery is totally charged.
6			ϕ	0	Change MPP for a value where the PV just injects the load power demand
7	$P_{PV} < P_{Load}$	SOC >20	ϕ	ϕ	Both PV and battery supply the load. In some cases, when these two cannot give the total energy to the load, it is purchased energy to the grid.
8		0 <SOC <20	Peak/Shoulder	ϕ	It is purchased energy from the grid to supply the load with the missing quantity.

V. SIMULATIONS AND RESULTS

This section presents the simulations and results of the proposed UPAC with its energy management system, shown in Fig. 1. Matlab/Simulink is used to verify the performance of the proposed UPAC. The PV array, with a peak power around 4kW, must supply a three-phase load located in a rural area in Tomar, Portugal. Since it is a low voltage application in a rural area, it was selected a RL overhead power line. According to EDP in [25], was decided for a cable LXS 4x16 with a length around 100m. Table IV depicts all the parameters used throughout this research work.

TABLE IV
PARAMETERS USED IN THE SIMULATIONS

	Parameter	**Value**
DC/DC buck boost	C_1	$2000\mu F$
	C_2	$980\mu F$
	L	$5.1mH$
	r_L	$51m\Omega$
MPPT Gains	k_{v_MPP}	-50
	k_I	$5.5 * 10^4$
	k_{vc1}	150
Inverter input and output filter parameters	C_{DC}	$820\mu F$
	r	$1m\Omega$
	L_{IF}	$33mH$
	C_{IF}	$1\mu F$
Invert er control gains	k_{ii}	130
	k_{pi}	0.2
	k_{iv}	-1
	k_{pv}	-0.05
Equivalent Capacitor	C_B	$8100F$
Reversible buck-boost converter's output filter	L_B	$12mH$
RL electric power line	l	$0.1km$
	R_{20C}	0.19Ω
	L_{line}	$0.03mH$

A. Effect of Partial Shading

In order to simulate the impact of the partial shading in the proposed UPAC, it was considered an isolated PV array supplying a resistive load. The PV array configuration is the one presented in Fig. 2 with 12 panels each one with its MPPT. To validate the choice of this structure, a second simulation was also made using just two MPPTs (a single MPPT for each set of 6 PVs). The two structures are compared under the same conditions. The area of 4 panels under PSC was considered. Table V presents the solar radiations applied in the two simulations, under a cell temperature of 25ºC.

TABLE V
IRRADIANCES APPLIED IN EACH PV MODULE

Panel	PV1	PV2	PV3	PV4	PV5	PV6	PV7	PV8	PV9	PV10	PV11	PV12
G[W/m^2]	800	1000	1000	1000	1000	1000	600	600	800	1000	1000	1000

Figures 8 and 10 show the results for the first situation where each module has its own MPPT. The analysis allows us to conclude that changing the irradiance will mostly affect the PV current, as seen in Figure 10. Consequently, the MPP decreases and, consequently, the power injected by each panel decreases, too. In this simulation the total power injected on the load is around 3.473 kW, instead of 4 kW. Despite under PSC, it is also observed that each MPPT can track the correspondent MPP, compared with the ones of the PV datasheet.

Otherwise Figures 9 and 11 show the simulation with each string of 6 panels connected to one MPPT. As can be seen, in this case, the MPPTs have difficulty tracking the exact point where the power is maximum. For instance, the output voltage of PV2 is higher than 60V, instead of 59.7V, meaning that the selected voltage is not the one in the MPP.In addition, for PV1 in this second situation the voltage value ($V_{PV1} \approx -105\ V$) no

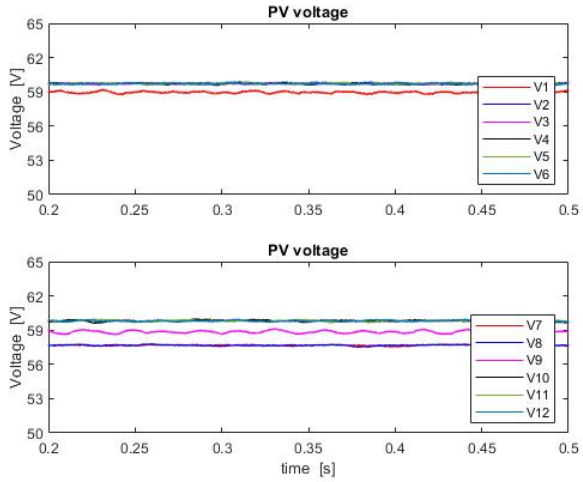

Fig. 8. PV voltages with 12 MPPTs

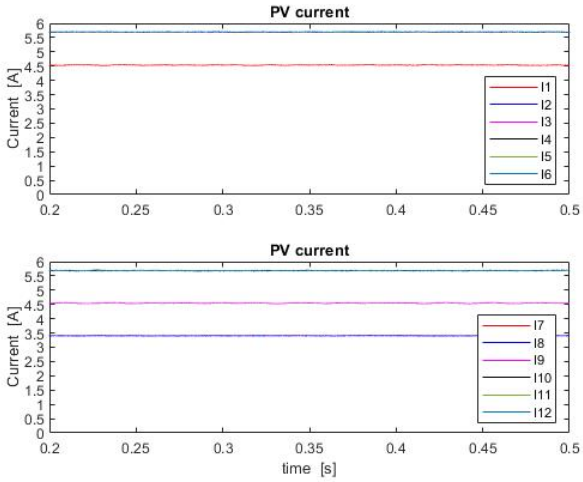

Fig. 10. PV currents with 12 MPPTs

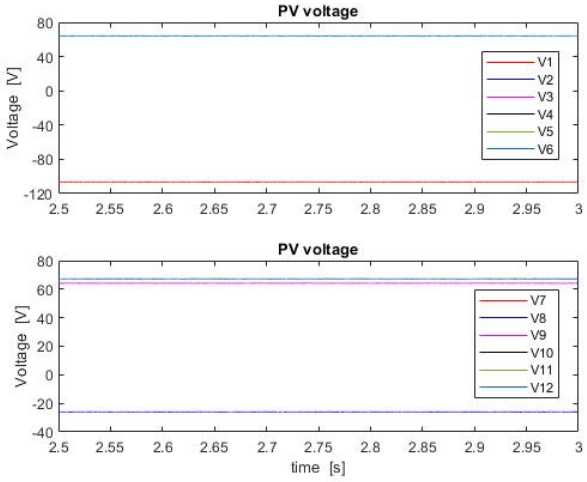

Fig. 9. PV voltages with 2 MPPTs

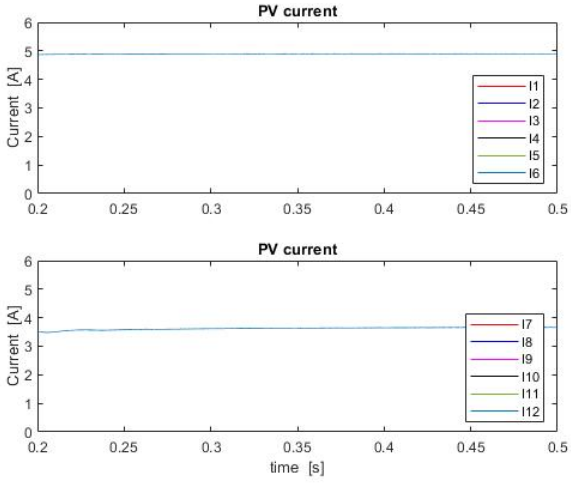

Fig. 11. PV currents with 2 MPPTs

longer makes sense (meaning the PV model loses its validity), which comparing with the previous situation in Fig. 8 V_{PV1} was equal to 59 V. The total power reached was 1.82kW, which is much lower than the one obtained with 12 MPPTs.

Therefore, it is concluded that in PSC it is advantageous to use an MPPT for each PV module than 2 MPPTs for two sets of paralleled six modules in series. Indeed, in the first situation the MPPTs can first optimize the MPP for each panel. This means that the tracker has just one point in a convex function to find where the power is maximum. However, in the second situation, the 2 MPPTs have to find an MPP from a set of different points where the power reaches a maximum (GMPP). As seen, the MPPTs can stay stuck in other points than GMPP.

B. Simulation of the Energy Management System

This subsection presents the results of the proposed UPAC in order to assess the energy management of the entire system. To verify the robustness of the systems to work at any time of the year, the system was simulated in summer and in winter during hours of high solar radiation (between 12:00 and 15:00). The case studies take into account the following points:

- To have reasonable simulation times, the 12 modules with MPPT are replaced by a single module, including a current source that injects the PV array power measured in a separated simulation under the same conditions but using the 12 modules with MPPT supplying a resistive load.
- The irradiance and ambient temperature values were taken from the European Commission's tool [26].
- The cell temperature was calculated as explained in [11], from the ambient temperature.
- The equivalent capacitor C_B value was divided by 3600s. As a result, one second of simulation corresponds to an hour of the entire system working. Otherwise, it would not be possible to make simulations long enough to

observe the capacitor charging/discharging.

- During the first 15min the PV is under PSC due to a passing cloud.
- The PV array output power P_{PV}, grid power P_{Grid}, load power P_{Load} and SOC curves are analysed.

Therefore, the performance of the energy management system, based on the rules shown in Table III, will be evaluated

The first case study considers a workday in June. The irradiance values are depicted in Table VI. The correspondent PV array output power P_{PV} as well as the load power demand P_{Load} are depicted in Table VII. The results are shown in Figures 12 and 13.

TABLE VI
CASE STUDY JUNE WORKDAY - IRRADIANCE (G[W/m^2]) IN EACH PV ($\theta_c = 49.5$ºC)

Panel	PV1	PV2	PV3	PV4	PV5	PV6	PV7	PV8	PV9	PV10	PV11	PV12
12:00 - 12:15	500	500	550	550	550	600	500	500	550	550	550	600
12:15 - 13:00							825					
13:00 - 14:00							800					
14:00 - 15:00							720					

TABLE VII
CASE STUDY JUNE WORKDAY - PV ARRAY OUTPUT POWER AND LOAD POWER ($SOC_i = 30\%$)

Hour	12:00 - 12:15	12:15 - 13:00	13:00 - 14:00	14:00 - 15:00
P_{PV}[W]	1860	2950	2850	2540
P_{Load}[W]	3000	3000	1000	500

As can be seen in figure Figure 12, during the first 15min the PV injected power is lower than the needed power by the load. In addition, as $SOC > 20\%$, the application of the seventh rule is verified. As a result, the SOC decreases meaning that the equivalent capacitor is discharging. Between 12:15 and 13:00, the energy management system follows exactly as in the first 15min. However, it is noted that, the larger difference is between the PV power and the load power, the faster the discharging of the battery is. As a result, during this period the battery is discharging more slowly. In the last two hours, the system works following the fourth rule: $P_{PV} > P_{Load}$ and $SOC < 80\%$ and, as a consequence the panel supplies the load and the battery is being charged. Over these three hours, the grid power remains approximately zero (neither supply nor receive).

The second case study considers a workday in December. Table VIII depicts the amount of solar radiation that reaches each panel. Table IX shows the correspondents P_{PV} and P_{Load} and Figures 14 and 15 the results.

TABLE VIII
CASE STUDY DECEMBER WORKDAY- IRRADIANCE (G[W/m^2]) IN EACH PV ($\theta_c = 30$ºC)

Panel	PV1	PV2	PV3	PV4	PV5	PV6	PV7	PV8	PV9	PV10	PV11	PV12
12:00 - 12:15	200	200	250	250	250	300	200	200	250	250	250	300
12:15 - 13:00							580					
13:00 - 14:00							545					
14:00 - 15:00							450					

TABLE IX
CASE STUDY DECEMBER WORKDAY- PV ARRAY OUTPUT POWER AND LOAD POWER ($SOC_i = 30\%$)

Hour	12:00 - 12:15	12:15 - 13:00	13:00 - 14:00	14:00 - 15:00
P_{PV}[W]	830	2140	2000	1630
P_{Load} [W]	3000	3000	1000	500

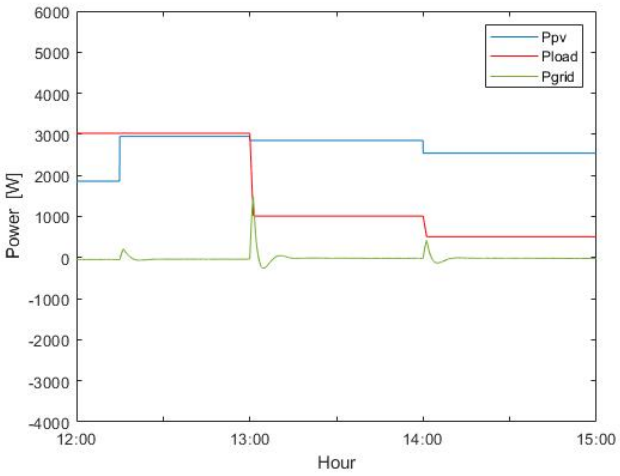

Fig. 12. Case Study June Workday: P_{pv},P_{Load} and P_{grid} [W]

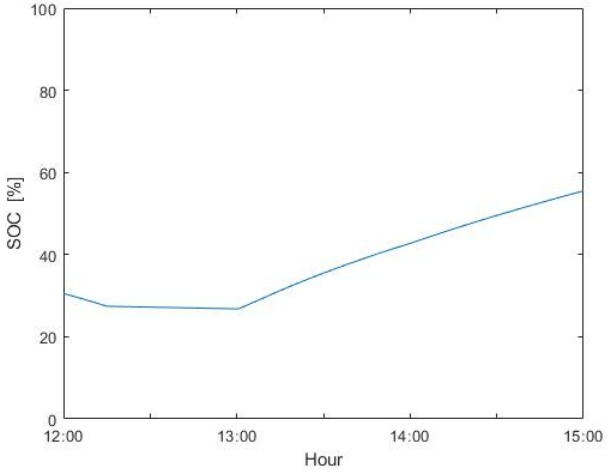

Fig. 13. Case Study June Workday: SOC [%]

Analysing Figure 14 are depicted three different situations along the first hour. During this time $P_{PV} < P_{Load}$. Between 12:00 and 12.15, the load is supplied by the PV array, the battery and grid (P_{Grid} negative means is injecting). Therefore, the SOC decreases and it is purchased energy to the the grid (it is been applied the seventh's rule). It is noted that, the power that the grid is injecting on the system is increasing with the decreasing of the SOC. Between 12:15 and 12:45, the PV injects the total power in the load and the battery can inject the remaining until to be total discharged (at 12:45). Finally, in the last 15min, the $SOC = 20\%$ and so, there is no more energy available in the storage system (eight's rule). Consequently, the load is supplied by the PV array and the grid ($P_{grid} = P_{PV} - P_{Load}$). Furthermore, between 13:00 and 15:00 , $P_{PV} > P_{Load}$ and the system follows the fourth rule (load is totally supplied by the PV array and battery is charging).

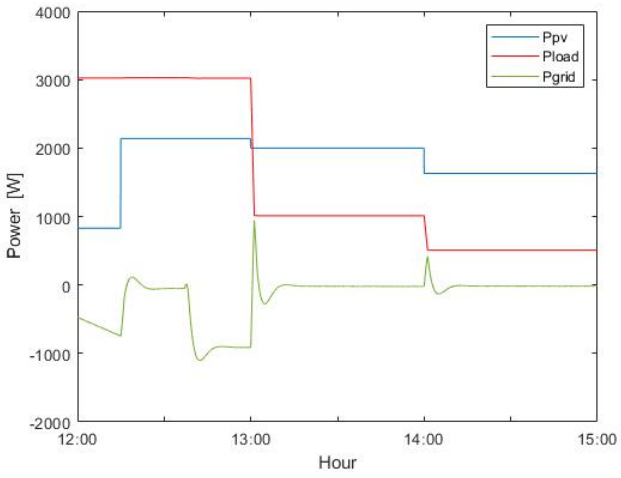

Fig. 14. Case Study December Workday: P_{pv},P_{Load} and P_{grid} [W]

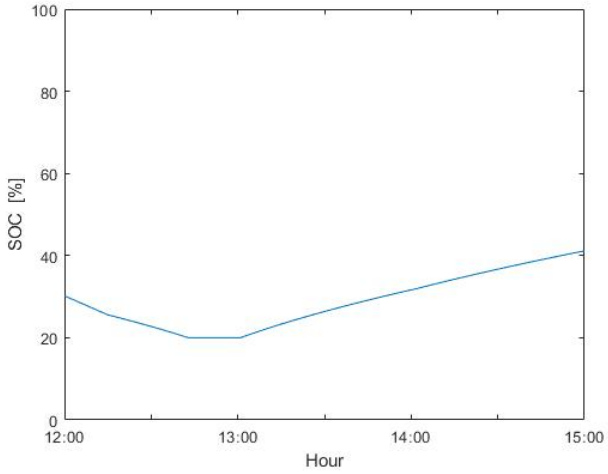

Fig. 15. Case Study December Workday: SOC [%]

C. Three-phase inverter DC voltage control

In order to verify if the inverter control is working, the voltage V_{CDC} (in the capacitor C_{DC} terminals in Figure 1) should be analysed. This voltage should keep constant.

Therefore, considering the June workday, Fig. 16 depicts V_{CDC} during a short time of that simulation. It turns out that the inverter control can track the expected voltage (700V) and keep it constant. Nevertheless, it can be observed that some peaks appear when perturbations are applied to the PV power output and load power, but controllers kept the disturbances small (<12%) and short lived (<100ms). Fig. 16 illustrates one of these peaks. When P_{Load} decreases to 500W, a peak in V_{CDC} emerges (decreases from 700V to around 645V). After 0.1s, the voltage increases and stabilizes again in 700V. The voltage disturbance in V_{CDC} depends not only on the difference between the powers (P_{PV} and P_{Load}), but mainly on the steepness of that difference.

As well as the inverter output AC currents must be analysed since the inverter control uses internal current control (shown in Fig. 17). It is expected that the currents keep constant in a certain value which guarantees the voltage V_{CDC} tracks the reference one. Before the perturbation being applied, the current RMS value keep constant around the 7A. When P_{Load} decreases, the currents decreases. After 0.1s, the currents stabilize in a new value, around the RMS value of 3A . This value is lower than the one before the perturbation since the load power demand decrease.

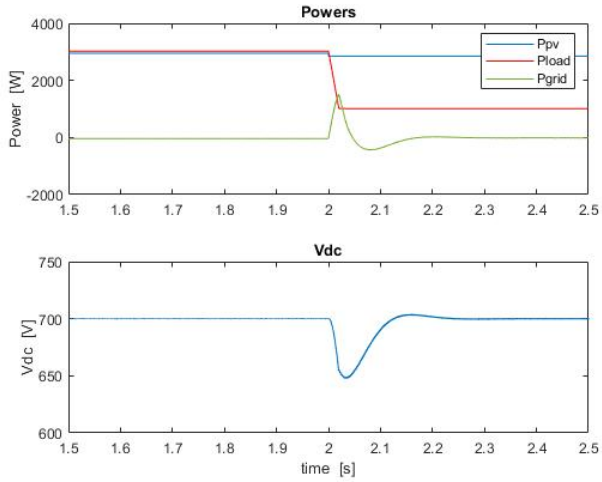

Fig. 16. Inverter input voltage V_{CDC} behaviour

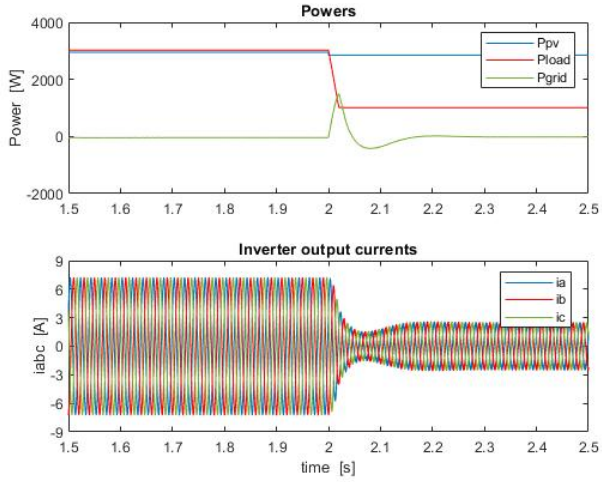

Fig. 17. Output currents behaviour

VI. Conclusions

The main objective of this dissertation was the design and simulation of an UPAC with PV microgenerators, ESS integration and grid-connection, to operate under PSC.

In a first test, it was concluded that for the PV structure implemented (2 parallel strings of 6 panels in series) the best approach is to use a MPPT for each module under PSC. In the PSC test, the resulting PV array output power was 3.473kW, in comparison with 1.82kW when the common approach of 2 MPPT (one for each set of 6 modules) was

just used. Thus, using a MPPT for each module it is possible to maximize the power generated by each panel. Additionally, the results demonstrated that the combination between backstepping algorithm, and the incremental conductance algorithm used to generate the reference voltage, resulted in an accurate tracking of the expected MPP. For instance, for an irradiance of 1000W/m^2 the PV output voltage was 59.7V, equal to the one at the MPP.

To verify the performance of the entire system while working, the entire energy management system was simulated. The primary aim was to guarantee that the load was totally supplied in any time of the year, in accordance with a table of rules. Two different situations were tested between 12:00 and 15:00, under a 15min passing cloud:

- In June workday case study - the P_{PV} was 1.86kW. With a load of 3kW, the load is supplied by the PV array and the battery. As result, the battery discharged from 30% to 25% (7th rule). After the shading, the P_{PV} changed to 2.95kW and the load power remains 3kW and, as result, the system works in the same rule although the battery supplies much less power. Of course, the larger difference is between the PV power and the load power the faster the discharging of the battery is, whereas if that power difference is negative the battery charges. When the load decreases to 1kW and thus, the load was totally supplied by the PV array and the battery was charging from 25% to 55% (4th rule).
- In December workday case study - the P_{PV} was 0.83kW. With a load of 3kW, the power is shared by the PV array, battery and also the grid (7th rule). It means that in this situation the customer needs to purchase energy to the gird. I is noted that, the power that the grid is injecting on the system is increasing with the decreasing of the SOC. After the shading, during a certain period the P_{PV} was 2.14kW and the load still 3kW and so the 8th rule was applied. It means the battery was discharged (20%) and the grid was injecting a constant energy (equal to $P_{PV} - P_{Load}$). Then, the P_{Load} decreases to 1kW and the system applied the 4th rule.

The final test consisted in observing the three-phase inverter operation. As a result, the linear control implemented successfully tracked the expected DC voltage of 700V and the inverter output currents. It is also noted that, during the first seconds when a perturbation is applied, a transient was observed. Nevertheless, the system was able to fully recover its stability in less than 0.1s, even under shading conditions.

REFERENCES

[1] K. Ali, L. Khan, Q. Khan, S. Ullah, S. Ahmad, S. Mumtaz, and F. W. Karam, "Robust integral backstepping based nonlinear mppt control for a pv system," 2019.

[2] International Energy Agency, "Market Report Series: Renewables 2018," last accessed 19 June 2020.

[3] P. Dondi, D. S.-E. Bayoumi, C. Haederli, D. Julian, and M. Suter, "Network integration of distributed power generation," 2002.

[4] Ministério Do Ambiente Ordenamento Território Energia, "Decreto-Lei n.º 153/2014," in *Diário da República - I Série*, 2014, pp. 5298–5311.

[5] N. Femia, G. Petrone, G. Spagnuolo, and M. Vitelli, "Optimization of perturb and observe maximum power point tracking method," *IEEE Transactions on Power Electronics*, vol. 20, pp. 963–973, 2005.

[6] M. A. Elgendy, B. Zahawi, and D. J. Atkinson, "Assessment of the incremental conductance maximum power point tracking algorithm," *IEEE Transactions on Sustainable Energy*, vol. 4, pp. 108–117, 2013.

[7] A. K. Podder, N. K. Roy, and H. R. Pota, "Mppt methods for solar pv systems: A critical review based on tracking nature," *IET Renewable Power Generation*, vol. 13, pp. 1615–1632, 2019.

[8] K. Ishaque, Z. Salam, A. Shamsudin, and M. Amjad, "A direct control based maximum power point tracking method for photovoltaic system under partial shading conditions using particle swarm optimization algorithm," *Applied Energy*, vol. 99, pp. 414–422, 2012.

[9] Panasonic, "N340 HIT® + Series," last accessed 16 July 2020. [Online]. Available: https://na.panasonic.com/us/energy-solutions/solar/hit-series/n340-hitr-series

[10] F. A. Pereira Lourenço, "Maximum Power Point Tracking in Photovoltaic Systems with Partial PV Shadowing," Master's thesis, Master's Thesis, Instituto Superior Tecnico, 2018.

[11] R. Castro, *Uma Introdução às Energias Renováveis: Eólica, Fotovoltaica e Mini-Hídrica*. IST Press, 2012.

[12] F. Labrique and J. Santana, *Electrónica de Potência*. Edições da Fundação Calouste Gulbenkian, 1991.

[13] M. K. Kazimierczuk, *Pulse-width modulated DC-DC power converters*. John Wiley & Sons, 2016.

[14] D. Czarkowski, "10-DC-DC Converters," in *Power Electronics Handbook*, 4th ed., M. Rashid, Ed. Butterworth-Heinemann, 2018.

[15] M. Boujmil, A. Badis, and M. Nejib Mansouri, "Nonlinear robust backstepping control for three-phase grid-connected pv systems," 2018, last accessed 8 September 2020.

[16] S. F. Silva, José Fernando Pinto, "35 - Linear and Nonlinear Control of Switching Power Converters," in *Power Electronics Handbook*, 4th ed., M. Rashid, Ed. Butterworth-Heinemann, 2018.

[17] A. D. Martin, J. M. Cano, J. F. Silva, and J. R. Vazquez, "Backstepping control of smart grid-connected distributed photovoltaic power supplies for telecom equipment," *IEEE Transactions on Energy Conversion*, vol. 30, pp. 1496–1504, 2015.

[18] H. Khalil, *Nonlinear Systems Third Edition*. Prentice Hall, 2002.

[19] J. F. A. Silva, *Electrónica Industrial: Semicondutores e Conversores de Potência*, 2nd ed. Fundação Calouste Gulbenkian, 2013.

[20] S. Silva, Fernando Pinto and J. Santana, *Conversores Comutados para Energias Renováveis*. Unpublished, 2016.

[21] H. Abdi, B. Mohammadi-ivatloo, S. Javadi, A. R. Khodaei, and E. Dehnavi, "Energy Storage Systems," in *Distributed Generation Systems: Design, Operation and Grid Integration*. Elsevier, 2017, last accessed 10 June 2020.

[22] EDP Comercial, "O QUE É A OPÇÃO HORÁRIA E QUAL A MELHOR PARA MIM?" last accessed 19 June 2020. [Online]. Available: https://www.edp.pt/particulares/apoio-cliente/perguntas-frequentes/pt/contratos/novo-contrato/o-que-e-a-opcao-horaria-e-qual-a-melhor-para-mim/faq-4823

[23] A. S. Alcobia, "Regulação de Tensão nas Redes de Baixa Tensão auxiliada por Microprodutores," Master's thesis, Master's Thesis, Instituto Superior Tecnico, 2015.

[24] F. Bernardes, "Compensação de sobretensões originadas por sistemas de microgeração em redes de baixa tensão," Master's thesis, Master's Thesis, Instituto Superior Tecnico, 2014.

[25] EDP Distribuição, "Ligação de clientes de baixa tensão," 2018, last accessed 15 July 2020. [Online]. Available: https://www.edpdistribuicao.pt/sites/edd/files/2019-10/DIT-C14-100.pdf

[26] European Comission, "Daily radiation," last accessed 25 June 2020. [Online]. Available: https://ec.europa.eu/jrc/en/PVGIS/tools/daily-radiation